VIP Dye-Sensitized Solar Cells

DOI: 10.1002/anie.201104786

Low-Cost Copper Zinc Tin Sulfide Counter Electrodes for High-Efficiency Dye-Sensitized Solar Cells**

*Xukai Xin, Ming He, Wei Han, Jaehan Jung, and Zhiqun Lin**

Dye-sensitized solar cells (DSSCs) are among the most promising photovoltaic devices for low-cost light-to-energy conversion with relatively high efficiency.[1] A typical DSSC consists of three key components: a dye-sensitized semiconductor photoanode, an electrolyte with a redox couple (triiodide/iodide), and a counter electrode (CE). Upon photoexcitation, electrons generated from photoexcited dyes are injected into the conduction band of photoanode composed of TiO_2 and the dyes are regenerated by redox reaction with the electrolyte. Oxidized ions (triiodide) in the electrolyte then diffuse to the CE and are finally reduced to iodide at the surface of the CE. An ideal CE should possess high electrocatalytic activity for the reduction of charge carriers in electrolyte as well as high conductivity. To date, the most commonly used CE is fluorine-doped tin oxide (FTO) glass coated with a thin layer of platinum. However, as a noble metal, the low abundance (0.0037 ppm) and high cost (US$ 50/gram) prevent platinum from being used for large-scale manufacturing.[2]

In this context, considerable efforts have been made to replace Pt with abundant low-cost alternatives, including carbon-based materials (for example, carbon nanotubes, carbon black, and graphite),[3,4] conjugated polymers,[2,5] and inorganic materials as CEs. In comparison to carbon materials and polymers, inorganic compounds carry many advantageous characteristics, such as simple preparation and a diversity of materials that can be used.[6] In recent years, a variety of binary metal oxides,[7] metal sulfides,[8] metal nitrides,[4,9] and metal carbides[6] have been developed as CEs. To the best of our knowledge, the use of abundant ternary or quaternary materials as potential substitutes for Pt as low-cost CEs has not yet been explored.

A quaternary chalcogenide semiconductor, copper zinc tin sulfide (hereafter referred to as CZTS), is most widely known as one of the most promising photovoltaic (PV) materials, and it is widely used in thin-film solar cells.[2,10] Notably, CZTS is composed of naturally abundant elements in the Earth's crust and has very low toxicity: it is environmentally friendly compared to two high-efficiency thin-film solar cells with CdTe and $Cu(In_{1-x},Ga_x)S_2$ (CIGS) that have toxic elements (Cd) and rare metals (indium and gallium).[10] Recently, high-efficiency thin-film solar cells have been demonstrated based on the superior PV performance of CZTS as a p-type semiconductor owing to its direct band gap of 1.5 eV and a large absorption coefficient ($>10^4\ cm^{-1}$).[11,12] However, no studies have centered on the electrocatalytic activity of CZTS for use in DSSCs. Herein, we present, for the first time, that CZTS can be exploited as an effective CE material to replace expensive Pt, yielding a low-cost, high-efficiency DSSCs. It is noteworthy that a power conversion efficiency (PCE) of 7.37% was achieved by a simple process of spin-coating CZTS followed by selenization.[13] This efficiency was highly comparable to the DSSC prepared by utilizing Pt (PCE = 7.04%) as the CE under the same device configuration.

We employed a solution-base synthesis approach to prepare CZTS nanocrystals.[14] Specifically, copper, zinc, and tin precursors dissolved in oleylamine (OLA) were purified at 130 °C and heated to 225 °C in argon. Subsequently, a sulfur solution was rapidly injected and stirred at 225 °C for 1 h. The product was centrifuged to yield CZTS nanoparticles (see the Experimental Section). Figure 1 a,b shows scanning transmission electron microscope (STEM) images of CZTS nanoparticles. The nanoparticle diameter was approximately (15 ± 6) nm and the lattice constant was 0.31 nm, corresponding to the (112) plane, which was consistent with the XRD result (Supporting Information, Figure S1).[15] It is worth noting that compared to conventional costly and low-throughput high-vacuum sputtering and vapor deposition of CZTS, the ability to produce a CZTS nanocrystal dispersion (that is, a nanocrystal "ink") that can be sprayed and coated on surface and then thermally annealed into larger-grain thin film would substantially lower the manufacturing cost and allow high-throughput solar-cell production.[12,14–16] The CZTS ink was then either spin-coated or drop-cast onto the clean FTO glass and sintered at 540 °C for 1 h in selenium vapor. The morphologies of resulting CZTS films after sintering in Se vapor are shown in Figure 1 c,d. The thickness of the CZTS layer was approximately 180 nm for the spin-coated sample and 2.3 μm for the drop-cast sample, respectively. Cracks were clearly evident on the drop-cast sample sintered in Se vapor, which are due to the stress induced during the solvent evaporation (Supporting Information, Figure S2b). The compositions of CZTS nanocrystals before and after treatment with Se vapor (selenization to yield CZTSSe) were

[*] X. Xin, W. Han, J. Jung, Prof. Z. Lin
School of Materials Science and Engineering, Georgia Institute of Technology, Atlanta, GA 30332 (USA)
E-mail: zhiqun.lin@mse.gatech.edu
X. Xin, W. Han, J. Jung, Prof. Z. Lin
Department of Materials Science and Engineering, Iowa State University, Ames, IA 50011 (USA)
Dr. M. He
The Key Laboratory of Molecular Engineering of Polymers and Department of Macromolecular Science, Fudan University Shanghai, 200433 (P.R. China)

[**] We gratefully acknowledge support from the DOE Ames Lab Seed Funding.

Supporting information for this article is available on the WWW under http://dx.doi.org/10.1002/anie.201104786.

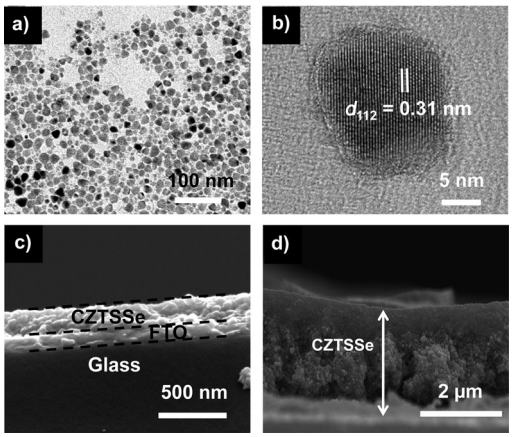

Figure 1. a) STEM image of CZTS nanocrystals. b) High-resolution STEM image; a nanocrystal was imaged along the [$\bar{1}$10] crystallographic axis. c,d) Cross-sectional FESEM images of c) spin-coated CZTS film after selenization and d) CZTS film drop-cast on FTO-coated glass after selenization.

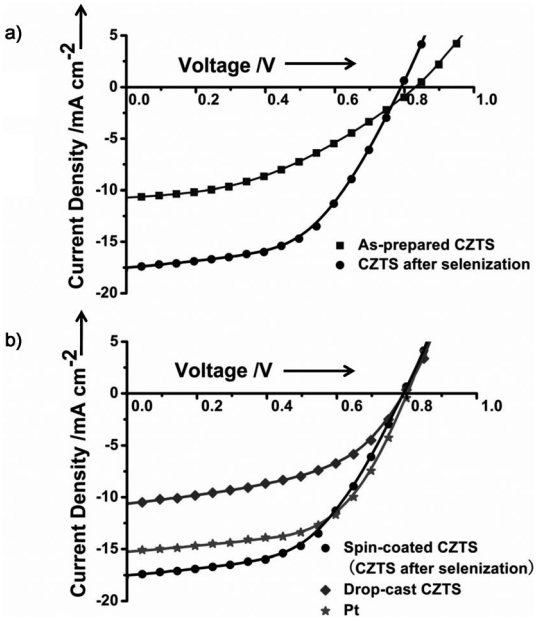

Figure 2. Photocurrent–voltage characteristics of DSSCs using CZTS or Pt films as CEs. a) As-prepared CZTS by spin coating but without sintering (■) and spin-coated CZTS film after selenization (CZTSSe; ●). b) Spin-coated CZTS film after selenization (CZTSSe; ●), drop-cast CZTS film after selenization (CZTSSe; ◆), and Pt film (★).

$Cu_{1.51}Zn_{1.00}Sn_{1.45}S_{3.61}$ and $Cu_{1.49}Zn_{1.00}Sn_{1.51}S_{0.85}Se_{4.78}$, respectively, as determined by energy-dispersive X-ray spectroscopy (EDS; Supporting Information, Figure S3). The excess amount of Se may originate from the deposition of elemental Se during the selenization process.

A 16 μm thick TiO_2 nanoparticle layer was deposited on FTO glass by doctor blade coating, followed by a $TiCl_4$ treatment and exposure to O_2 plasma and sensitized with N719 dyes. The CZTS-coated or CZTSSe-coated FTO substrate served as CE was assembled together with a dye-sensitized TiO_2 photoanode. The ionic liquid electrolyte (ES-004) was then injected between two electrodes (see the Experimental Section).

Table 1: Photovoltaic performance of DSSCs with different counter electrodes.[a]

Counter electrodes	Samples	V_{OC} [V]	J_{SC} [mA cm^{-2}]	FF [%]	PCE [%]	R_s [Ω]	R_{ct} [Ω]	CPE [μF]
CZTS	SC[b]; as-prepared[c]	0.84	10.7	40.3	3.62	23.2	2.8	1.9
CZTSSe	SC; selenized[d]	0.80	17.7	52.2	7.37	16.8	1.6	14.7
CZTSSe	DC[e]; selenized	0.80	10.6	47.9	4.07	24.9	4.9	4.6
Pt	sintered in air	0.81	15.4	56.8	7.04	15.3	7.7	3.6

[a] V_{OC} = open-circuit voltage; J_{SC} = short-circuit current density; FF = fill factor; PCE = power conversion efficiency; R_s = series resistance; R_{ct} = charge-transfer resistance. [b] SC = spin coating. [c] As-prepared = no sintering and selenization. [d] Selenized in Se vapor. [e] DC = drop casting.

Figure 2 and Table 1 compare the performance of several N719 dye-sensitized solar cells with different CEs. Clearly, when spin-coated CZTS sintered in Se vapor, forming CZTSSe, was employed as the CE, the highest PCE of 7.37% was obtained (Figure 2; Table 1). The photocurrent density J_{SC} increased significantly after the sintering process, from 10.7 mA cm^{-2} in as-prepared sample to 17.7 mA cm^{-2} in the selenized sample (Figure 2a). The CZTS nanocrystals directly after spin-coating were covered with a layer of organic ligands (OLA) as revealed by SEM (Supporting Information, Figure S5a). This organic layer hindered the charge transport within the CZTS film and the redox reaction of triiodide/iodide on the CZTS surface. After sintering at 540 °C, the organic ligand was removed as evidenced by TGA analysis and SEM measurements (Supporting Information, Figure S4, S5b). As a result, J_{SC} increased more than 50%. In stark contrast to the sample in which the CZTS CE was prepared by drop-casting followed by selenization to form CZTSSe (Figure 2b), the spin-coated samples exhibited a larger J_{SC}, and thus higher PCE. The observed low J_{SC} with drop-cast CZTSSe CE may be attributed to high resistance for charge transport owing to a much thicker film used. The thickness of drop-cast CZTSSe film was 2.3 μm, which was over 10 times thicker than the spin-coated counterpart. In thin-film solar cells where the CZTS was utilized as PV material, a thicker CZTS film promoted light harvesting and simultaneously reduced charge transport. Thus, an optimum thickness of 1–2 μm was identified for CZTS thin-film solar cells.[12,13] It is worth noting, however, that in the present study the CZTS film was exploited as a CE material, therefore a large light absorption efficiency was no longer an advantage. Consequently, high resistance for charge transport dominated and lowered J_{SC}. The DSSC obtained from the spin-coated CZTS film after selenization (Figure 2a,b) showed a remarkably comparable PCE of 7.37% to that of 7.04% in the Pt-coated DSSC (Figure 2b; Table 1), signifying that CZTS possessed a good electrocatalytic activity to reduce oxidized triiodide to iodide. Further improvement of the photovoltaic

performance is expected, as many parameters of the counter-electrode preparation (such as CZTS composition and the fabrication method) have not yet been optimized. We also note that rational treatment of the photoanode (such as adding a scattering layer) would further increase the efficiency of both CZTSSe-coated and Pt-coated solar cells; this is the subject of future work.

To further elucidate the electrochemical characteristics of CZTS electrodes, electrochemical impedance spectroscopy (EIS) measurements was performed on dummy cells with a symmetric sandwich-like structure between two identical electrodes, that is, CE/electrolyte/CE (see the Experimental Section). The Nyquist plots are shown in Figure 3. The high-frequency (corresponding to low Z') intercept on the real axis (Z' axis) represents the series resistance R_S. The semicircle in the high-frequency range results from the charge-transfer resistance (R_{ct}) and the corresponding constant phase-angle element (CPE) at the electrolyte/CE interface.[6] The semicircle in the low-frequency range (corresponding to high Z') arises from the Nernst diffusion impedance of the triiodide/iodide couple in electrolyte.[6] The values of R_s, R_{ct}, and CPE obtained by fitting the spectra in Figure 3 with an EIS spectrum analyzer are summarized in Table 1. The large R_s of as-prepared CZTS CEs and drop-cast CZTSSe CEs can be attributed to the presence of organic ligand on the CZTS surface and the large thickness, respectively. Among all samples, spin-coated CZTSSe CEs exhibited the smallest R_{ct} and largest CPE, suggesting a good catalytic activity and large surface areas.[6] The R_{ct} of CZTS and CZTSSe CEs were less than that of Pt CE, indicating a superior catalytic property of CZTS and CZTSSe. However, R_s of CZTS and CZTSSe CEs were larger than that of the Pt CE, which was most likely due to the relatively large conductivity of Pt as compared to semiconductor CZTS and CZTSSe. By reducing the thickness of CZTS and CZTSSe layers, and thereby reducing R_s, a further increase in the performance of solar cells may be enabled. The EIS results agreed well with the photocurrent–voltage experiments.

In summary, we have demonstrated a novel Pt-free CE for DSSCs based on low-cost quaternary CZTS nanocrystals. With a simple wet-chemistry synthesis of CZTS and a viable spin-coating fabrication of CE, the resulting CZTS film after selenization exhibited an impressive electrocatalytic performance as CEs to promote the regeneration of iodide from triiodide in electrolyte, yielding a PCE of 7.37%, which is remarkably similar to that of the Pt CE (PCE = 7.04%). The use of CZTS as CEs may expand the possibilities for developing low-cost and scalable DSSCs that dispose of the need for expensive and scarce platinum.

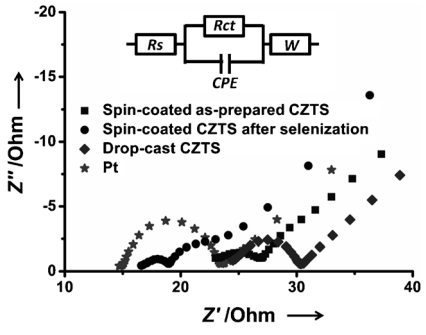

Figure 3. Nyquist plots of dummy cells with a symmetric sandwich-like structure between two identical electrodes consisting of: As-prepared CZTS by spin coating but without sintering (■), spin-coated CZTS film after selenization (CZTSSe; ●), drop-cast CZTS film after selenization (CZTSSe; ◆) and Pt (★). The frequency scan ranged from 0.1 Hz to 1 MHz. The corresponding circuit is shown in the inset.

Experimental Section

Synthesis of Cu_2ZnSnS_4 nanocrystals: Copper zinc tin sulfide (CZTS) was prepared according to the literature.[14] Copper(II) acetylacetonate (0.5 mmol, 99.99%, Sigma–Aldrich), zinc acetylacetonate (0.25 mmol, 99.995%, Sigma—Aldrich), and tin(IV) bis(acetylacetonate) dibromide (0.25 mmol, 98%, Sigma–Aldrich) were added to a three-neck round-bottom flask with oleylamine (OLA, 10 mL). The mixture was heated to 130 °C while purging with Ar for 30 min, and then the temperature was further increased to 225 °C. Sulfur in OLA (1M, 1 mL) was then injected to the mixture. The mixture temperature was kept at 225 °C for 1 h and then cooled down to 80 °C. The mixture was then diluted with toluene and the CZTS nanoparticles were precipitated with 2-propanol. Nanoparticles were separated by centrifugation at 4000 rpm for 5 min. After centrifuging, the supernatant was decanted and the precipitate was dispersed again in toluene. The alternating precipitation and dispersion process was repeated several times with 2-propanol and toluene to obtain the final product. The CZTS nanoparticles were finally dissolved in toluene and concentrated to 150 mM.

Fabrication of DSSCs: 3 mm thick FTO glass (15 $\Omega\,cm^2$) was cut into $2\times2\ cm^2$ pieces. The concentrated CZTS nanocrystal ink was coated on FTO glass by either spin-coating or drop-casting to form a nanocrystal thin film. The thickness of the CZTS layer prepared by spin-coating and drop-casting was 180 nm and 2.3 μm, respectively. Subsequently, the CZTS films were annealed at 540 °C in selenium vapor (to form CZTSSe. After selenization, the CZTSSe films were immersed into 3 wt% KCN aqueous solution to remove excess selenium. Pt-coated FTO glass was prepared by drop-casting 0.5 mM H_2PtCl_6/2-propanol solution on the clean FTO glass and subsequently sintering at 380 °C for 30 min. 25 nm TiO2 nanoparticles (P-25, Degussa) and poly(ethylene glycol) were dissolved in a mixture of deionized water and ethanol and stirred overnight to yield TiO_2 paste. A 16 μm thick TiO_2 nanoparticle layer was coated on the FTO glass. After sintering at 500 °C for 3 h and cooling down to 80 °C, the TiO_2 nanoparticle-coated FTO glass was immersed into 0.2 M $TiCl_4$ aqueous solution and kept in an oil bath at 70 °C for 1 h.[17] It was then annealed again at 500 °C for another 1 h. Finally, the TiO_2 photoanode was exposed to O_2 plasma for 10 min[17] and immersed in bis(tetra-*n*-butylammonium) *cis*-(diisothiocyanato)bis(2,2′-bipyridyl-4,4′-dicarboxylato)ruthenium(II) (N719, 0.2 mM, Solaronix) dye solution for 24 h. DSSCs with an active area of approximately 0.10 cm^2 were assembled together with the CZTS-coated, CZTSSe-coated, or Pt-coated FTO glass by applying a 60 μm thick hot-melt sealed film as the spacer (SX1170-25; Solaronix Co.). The redox electrolyte used in the study was an ionic liquid containing 0.60 M BMIM-I, 0.03 M I_2, 0.50 M TBP, and 0.10 M GTC in a mixture of acetonitrile and valeronitrile (v/v = 85/15) (No. ES-0004, purchased from io.li.tec, Germany). The electrolyte was injected between two electrodes. The dummy cells used for electrochemical impedance spectroscopy (EIS) analysis followed the same processes but with the photoanode changed to another counter electrode (CE).

Characterization: The size of CZTS nanocrystals was determined by transmission electron microscopy (JEOL 2100 scanning TEM, operating at 200 kV, MNIF at Iowa State University). The thickness and morphology of coated CZTS and CZTSSe films were imaged by a field-emission scanning electron microscope (FESEM; FEI Quanta 250 operating at 10 kV in high vacuum, same condition applied for

energy dispersive X-ray spectroscopy (EDS) analysis). The CZTS crystal size was measured by X-ray diffraction (XRD; SCINTAG XDS-2000, Cu K_α radiation ($\lambda = 0.154$ nm)). Oleylamine ligand removal from the CZTS surface was confirmed by thermogravimetric analysis (TGA; TA Instruments). Current–voltage (J–V) characteristics were measured using a Keithley Model 2400 multisource meter. A solar simulator (SoLux Solar Simulator) was used to simulate sunlight for an illumination intensity of 100 mW cm^{-2} as calibrated with a Daystar meter. Electrochemical impedance spectroscopy (EIS) analysis was conducted in dummy cells by using electrochemical test station (Novocontrol technologies). The frequency scan was from 0.1 Hz to 1 MHz and the spectra were fitted by software (EIS spectrum analyzer).

Received: July 9, 2011
Published online: September 7, 2011

Keywords: copper zinc tin sulfide · counter electrodes · dye-sensitized solar cells · energy conversion · photochemistry

[1] a) M. Grätzel, *Nature* **2001**, *414*, 338; b) B. O'Regan, M. Grätzel, *Nature* **1991**, *353*, 737; c) C. Xu, J. Wu, U. V. Desai, D. Gao, *J. Am. Chem. Soc.* **2011**, *133*, 8122; d) A. B. F. Martinson, T. W. Hamann, M. J. Pellin, J. T. Hupp, *Chem. Eur. J.* **2008**, *14*, 4458; e) M. Law, L. E. Greene, J. C. Johnson, R. Saykally, P. Yang, *Nat. Mater.* **2005**, *4*, 455; f) T. W. Hamann, R. A. Jensen, A. B. F. Martinson, H. Van Ryswyk, J. T. Hupp, *Energy Environ. Sci.* **2008**, *1*, 66; g) M. Ye, X. Xin, C. Lin, Z. Lin, *Nano Lett.* **2011**, *11*, 3214.

[2] S. Ahmad, J. H. Yum, H. J. Butt, M. K. Nazeeruddin, M. Grätzel, *ChemPhysChem* **2010**, *11*, 2814.

[3] J. E. Trancik, S. C. Barton, J. Hone, *Nano Lett.* **2008**, *8*, 982.

[4] G. R. Li, J. Song, G. L. Pan, X. P. Gao, *Energy Environ. Sci.* **2011**, *4*, 1680.

[5] T. N. Murakami, M. Grätzel, *Inorg. Chim. Acta* **2008**, *361*, 572.

[6] M. Wu, X. Lin, A. Hagfeldt, T. Ma, *Angew. Chem.* **2011**, *123*, 3582; *Angew. Chem. Int. Ed.* **2011**, *50*, 3520.

[7] C. S. Chou, C. M. Hsiung, C. P. Wang, R. Y. Yang, M. G. Guo, *Int. J. Photoenergy* **2010**, *2010*, 9.

[8] a) M. Wang, A. M. Anghel, B. Marsan, N.-L. Cevey Ha, N. Pootrakulchote, S. M. Zakeeruddin, M. Grätzel, *J. Am. Chem. Soc.* **2009**, *131*, 15976; b) H. Sun, D. Qin, S. Huang, X. Guo, D. Li, Y. Luo, Q. Meng, *Energy Environ. Sci.* **2011**, *4*, 2630.

[9] a) G. R. Li, F. Wang, Q. W. Jiang, X. P. Gao, P. W. Shen, *Angew. Chem.* **2010**, *122*, 3735; *Angew. Chem. Int. Ed.* **2010**, *49*, 3653; b) Q. W. Jiang, G. R. Li, X. P. Gao, *Chem. Commun.* **2009**, 6720; c) Q. W. Jiang, G. R. Li, S. Liu, X. P. Gao, *J. Phys. Chem. C* **2010**, *114*, 13397.

[10] S. E. Habas, H. A. S. Platt, M. F. A. M. van Hest, D. S. Ginley, *Chem. Rev.* **2010**, *110*, 6571.

[11] a) K. Ito, T. Nakazawa, *Jpn. J. Appl. Phys. Part 1* **1988**, *27*, 2094; b) H. Katagiri, K. Jimbo, W. S. Maw, K. Oishi, M. Yamazaki, H. Araki, A. Takeuchi, *Thin Solid Films* **2009**, *517*, 2455.

[12] T. K. Todorov, K. B. Reuter, D. B. Mitzi, *Adv. Mater.* **2010**, *22*, E156.

[13] Q. Guo, G. M. Ford, W.-C. Yang, B. C. Walker, E. A. Stach, H. W. Hillhouse, R. Agrawal, *J. Am. Chem. Soc.* **2010**, *132*, 17384.

[14] Q. Guo, H. W. Hillhouse, R. Agrawal, *J. Am. Chem. Soc.* **2009**, *131*, 11672.

[15] S. C. Riha, B. A. Parkinson, A. L. Prieto, *J. Am. Chem. Soc.* **2009**, *131*, 12054.

[16] a) C. Steinhagen, M. G. Panthani, V. Akhavan, B. Goodfellow, B. Koo, B. A. Korgel, *J. Am. Chem. Soc.* **2009**, *131*, 12554; b) M. G. Panthani, V. Akhavan, B. Goodfellow, J. P. Schmidtke, L. Dunn, A. Dodabalapur, P. F. Barbara, B. A. Korgel, *J. Am. Chem. Soc.* **2008**, *130*, 16770.

[17] J. Wang, Z. Lin, *Chem. Mater.* **2010**, *22*, 579.

